UC Berkeley
UC Berkeley Previously Published Works

Title
Pore-level investigation of foam/oil interactions in porous media

Permalink
https://escholarship.org/uc/item/31k1d4m8

Journal
SPE Reservoir Engineering (Society of Petroleum Engineers), 5(4)

ISSN
0885-9248

Authors
Manlowe, DJ
Radke, CJ

Publication Date
1990

DOI
10.2118/18069-pa

Peer reviewed

eScholarship.org Powered by the California Digital Library
University of California

A Pore-Level Investigation of Foam/Oil Interactions in Porous Media

David J. Manlowe· and Clayton J. Radke, SPE, U. of California

Summary. Direct visual studies of foam flow in etched-glass micromodels containing residual oil demonstrate that foam decays as a. result of breakage of pseudoemulsion films. Foam films collapse whenever nearby thin aqueous films separating gas bubbles and 011 rupture. Consequently, surfactant formulation for foam insensitivity to oil in porous media should be based on stabilizing pseudoemulsion films.

Introduction

Recently, use of foam as a mobility-control agent in EOR has shown success in steamflooding field applications.[1-5] Foam has the unique attribute of exhibiting apparent viscosities up to 1,000 times greater than its constituent phases: liquid and gas. To achieve and maintain mobility control in oil reservoirs, the foam should remain stable against collapse. Unfortunately, oil deleteriously affects the stability of foam,[6-11] which has obvious ramifications for the use of foam in EOR.

For the most part, foam/oil interactions in porous media have been characterized by studies on bulk foams. Typically, different variants of the common shake test are used in which surfactant solution, air, and oil are mixed to produce a foam, after which the decay of foam height is measured over time. The rate at which the foam height decays is thought to be a measure of the ability of the surfactant to produce and stabilize foam in the presence of the sample oil. This result may indeed be valid for bulk foams. However, direct application to foams in porous media is suspect. The type of foam present in a shake test may be radically different from that in porous media, especially with regard to the foam structure, the thickness of the lamellae, and the processes by which the foam collapses.[12] Nevertheless, the shake test is commonly used to screen surfactants for use in steam and CO_2 floods.[13]

Assessing the mechanistic interactions of foam and oil in porous media demands studies other than those on bulk foam outside the medium. Foam confined in a porous medium is different from bulk foam.[12,14,15] To date, the only method used to study foam stability against oil in porous media is to measure indirect properties such as pressure drops and foam-propagation rates across a core. Unfortunately, these secondary diagnoses have limited value for revealing the relevant interactions between foam and oil.

The objective of this work is to determine directly the mechanism(s) by which oil destabilizes foam in porous media. We visually studied foam in an etched-glass, porous-medium micromodel containing residual oil. The ability to create and analyze the foam in a transparent, prototype porous medium avoids the pitfalls of correlating results from bulk foam and secondary

parameter studies and provides pore-level information on actual destabilizing events.

Previous work

The strong destabilizing effect of crude oil on foam was first emphasized in the context of porous media by Bernard and Holm.[16] They reported that foam's effectiveness in reducing gas mobility greatly diminished when crude oil was present.

More recently, Lau and O'Brien[17] studied oil/foam interactions in laboratory sandpacks 90% saturated with oil at ambient temperature and pressure. The surfactant solution was a 0.5 wt% solution of Siponate DS-IO™ (a branched-side-chain dodecylbenzene sodium sulfonate) in 1.2 wt% NaCl. They selected oils that did not scavenge surfactant or form macroemulsions: hexadecane and a 30/70 mixture of Nujol™ and Shell-Sol 71™. Surface tension and interfacial tension (1FT) measurements between the phases revealed spreading coefficients of 1.8 and -0.8 mN /m for hexadecane (spreading oil) and for the Nujol mixture (nonspreading oil), respectively.

Lau and O'Brien reported that both foam formation and subsequent foam propagation was much slower for the spreading-oilsaturated sandpack than for the nonspreading oil. Also, the overall pressure response in the nonspreading-oil case occurred about two times faster than in the sandpack containing spreading oil. They concluded that spreading oils are more destabilizing to foam in porous media than nonspreading oils.

Nikolov et at.[10] studied bulk-foam/oil interactions microscopically. They concluded that the interactions are complex and that any number of contributing factors may lead to the destabilizing effect of oil. For their bulk foams in contact with oil, they did note that the stability of water films that form between oil drops and the gas phase (i.e., pseudoemulsion films) can play an important role in the overall system stability.

Jensen and Friedmann[18] studied the propagation rates of nitrogen and steam foams at 149°C in partially oil-saturated Berea sandstone cores. Three unnamed surfactants, all diluted to 0.5 active wt% in a synthetic brine solution (0.1 wt% NaCl and 0.05 wt% $CaCl_2$), were studied with four crude and two synthetic oils. Phase partitioning and thermodegradation were minimal for all the surfactants. Preformed foam was injected into a 25%-oil-saturated sandstone, allowing detailed study of the effect of oils on the foam-propagation process.[18]

Jensen and Friedmann concluded that the type of oil had little effect on the overall propagation rate of the different foams, but that the type of surfactant had dramatic effects. The surfactant labeled "oil-insensitive" produced a foam in all cases that propagated through the medium more rapidly than the other "oil-sensitive" surfactants. The pressure drop associated with the foam created with the oil-insensitive surfactant responded more rapidly than did the foams ofthe other surfactants. Further,

the difference in propagation rate and pressure response varied drastically among the different surfactant-stabilized foams.

Jensen and Friedmann also studied the effect of oil-saturation level on foam propagation. They varied the initial oil saturation between 25 and 35 % and found that for the oil-sensitive surfactants, oil had to be produced from the core before the foam could propagate.

This previous work suggests several foam destabilization mechanisms by resident oil, including the following.

1. Oil (and/or rock) scavenges surfactant from the gas/water interface.[9]

2. Oil/water macroemulsions form that deplete surfactant from the gas/water interface.[9]

3. Polar components in the oil preferentially adsorb at the gas/water interface, displacing or inactivating the more strongly stabilizing surfactants.[17]

4. Oil causes the water-wet rock to become oil-wet, which destabilizes the foam.[8]

5. Oil blocks the formation of foam by residing in germination sites (i.e., strategic bubble snap-off sites[14,18]).

6. Oil disrupts the orderly, stabilizing arrangement of micelles within the foam lamellae.[10]

7. Oil spreads at the gas/water interface, inducing lamella thinning and/or decreasing the critical capillary suction pressure for rupture.[17,19]

Even for nonpolar oils and surfactant-pre-equilibrated oil, water, and rock phases, foam still breaks. Therefore, Mechanisms 1 and 3 cannot be general, although loss of surfactant certainly will destabilize foam. Also, oil destabilizes foam in systems that are strongly water-wet and in systems that do not form strong macroemulsions, negating the generality of Mechanisms 2 and 4.

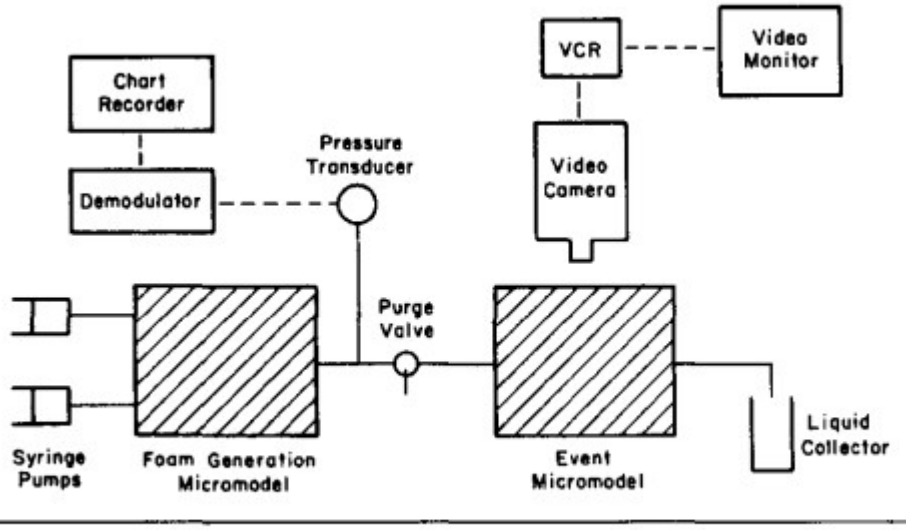

Fig. 1—Schematic of the foam-flow apparatus.

TABLE 1—EFFECT OF OIL SPREADABILITY ON BREAKTHROUGH TIME

System*	$S_{o/w}$** (mN/m)	Breakthrough Time (PV)
AOS 1416, 0.5 wt% NaCl, dodecane†	3.1	44
AES 911-2.5S, no salt, dodecane	8.6	52
AOS 1416, 0.05 wt% NaCl, dodecane	−0.2	57
AES 1215-12S, no salt, dodecane	3.0	64
AOS 1416, no salt, dodecane	8.1	69
AOS 1416, no salt, hexane	−2.2	91
X2101, no salt, dodecane	−4.9	110
Chaser SD1000, no salt, dodecane	−4.0	>200

*0.5 active wt% surfactant solutions equilibrated with the oil.
**Positive values of $S_{o/w}$ indicate spreading and negative values indicate lens formation.
†The event micromodel contains 30% residual saturation of the oil listed.

The destabilizing effect of oil on foam is evident even when the foam is pregenerated outside the porous medium. Therefore, the main mechanism for destabilization cannot be the blocking effect on the generation of foam suggested by Mechanism 5. Disruption of a structured order of micelles within a lamella (Mechanism 6) probably is not a generic mechanism because oil destroys foam at surfactant concentrations below the critical micelle concentration (CMC).

In light of these observations, it is obvious why the spreading mechanism (Mechanism 7) has received the most widespread acceptance. Studies with bulk foams are unlikely to yield definitive information on how oil actually breaks lamellae in porous media. Therefore, we chose to examine the spreading destabilization mechanism directly in a transparent, porous-medium micromodel.

Experiment

Apparatus and Procedures.

The process of fabricating etched-glass, porous-medium micromodels is now fairly well developed. The micromodels used here were fabricated by Adobe Labs (Socorro, NM) from a thin-section of a Kuparuk sandstone (Prudhoe Bay, AK). Our final micromodel incorporates three parallel inlet ports and one outlet port through which fluids enter and exit. A tangential (to flow direction), 150-μm-wide channel is etched into both ends of the etched-medium portion to ensure even distribution of fluids and to minimize fingering to the outlet port. The etched area is 7 cm in the axial flow direction and 4 cm across. The vertical height of the pores ranges from about 75 to 125 μm, according to data provided by Adobe Labs. Pore-throat and pore-body dimensions, ascertained by examining the pores under a microscope, are 25 to 100 μm and 150 to 300 μm, respectively.

The liquid-phase permeability of the micromodel, determined by measuring the pressure-droplflow-rate response for distilled water, is 1.1 ±0.15 μm^2, assuming a uniform pore height of 100 μm. Measurement of the total PV proved to be difficult because of the extremely small size of the model. Manlowe[20] details the novel conductimetric technique used to determine accurately an etchedporous-medium PV of 0.19±0.03 cm^3. This number includes only the volume of the etched area representing the porous medium. Finally, the effective porosity of the micromodel was calculated as 0.42, again assuming an average pore height of 100 μm.

The experimental flow apparatus (Fig. 1) consists of two essentially duplicate micromodels. Foam is pregenerated in the upstream model, while both qualitative and quantitative analysis of foam stability is conducted in the downstream model. Two syringe pumps (Harvard, Model 975) separately deliver air and aqueous surfactant solution to the foam-generation micromodel at 0.017 and 0.061 cm^3/min, respectively. This produces foam of 80% quality (the volume fraction of gas exiting the generation micromodel)

with a frontal advance rate (interstitial velocity) of about 19 m/d. Attempts to reduce the flow velocities with the Harvard pumps proved unsuccessful. The upstream foam-generation micromodel is attached by a T-joint to both a pressure transducer (Validyne, Model DPI2) and the downstream event micromodel.

The event micromodel is fixed prone on a movable microscope stand that admits exact measurement of *x* and *y* positions with precision micrometers. The range of the translational stage permits an entire view of the micromodel by a stationary camera with attached bellows (Silge and Kohne, Model Othoput 1198) and lens (Leitz Wetzlar, Model Summar f = 8 cm). With this assembly, both pore-level and overall views are possible with good resolution. The output of the camera is recorded by a VCR (Panasonic, Model AG6010) and displayed on a high-resolution color television monitor (Sony, Model PVM-127IQ-1371QM). The VCR allows real-time monitoring at 1/30 s/frame as well as slow-motion taping of events for future analysis.

The procedure was first to saturate the event micromodel completely with aqueous surfactant solution, to displace with oil to connate water saturation, and to waterflood at low capillary number (3×10^{-6}) to residual oil saturation (ROS). ROS was determined by tedious analysis of about 50 representative micrographs to be about 30% in all experiments. Next, gas and liquid were supplied to the foam-generation micromodel and exited to the atmosphere until a steady foam texture and quality were produced. Bubble size varied considerably, with an average length of around 75 μm. Finally, foam was injected into the event micromodel and the pressure drop was recorded until steady state was attained. In addition to copious pore-level visual analysis, the number of PV's injected into the event micromodel before foam production at the outlet was noted. Foam breakthrough time establishes a measure of foam stability in the presence of oil for a given surfactant/oil system. More detail on the experimental apparatus and procedures is available in Ref. 20.

Chemicals and Properties.

Two simple alkane oils, hexane (Aldrich, GLC, 96.5%) and dodecane (Eastman, GLC, 99+ %), and five different commercial anionic surfactants-AOS 1416 (Bioterg 40, Stepan Chemical Co., an alpha olefin sulfonate with a chain length of 14 to 16), AES 911-2.5S (Enordet, Shell Development Co., an alcohol ethoxysulfate with a chain length of 9 to 11 and 2 to 3 ethoxyl groups), AES 1215-12S (Enordet, Shell Development Co., an alcohol ethoxysulfate with a chain length of 12 to 15 and 12 ethoxyl groups), X2101 (Enordet, Shell Development Co., a linear alcohol ethoxysulfonate,[13] and Chaser SDlOOO (Chevron Chemical Co., an alkyl sulfonate dimer with an average chain length near 20)-were used in this study. The surfactants were prepared in 0.5 active wt% solutions, a concentration 1.5 to 3 times above the CMC. In all experiments, the oil and aqueous surfactant phases were pre-equilibrated by mild stirring for 2 days.

Ambient-temperature surface tensions of both oil and water solutions against air were determined by the Wilhelmy-plate technique using a Roller-Smith precision balance (Bipolar Corp., Model LG) and a 2.54-cm perimeter platinum plate. Each measurement is the average of at least five separate determinations. IFT's were measured by the drop-weight technique with oil droplets produced from a U-shaped, stainless-steel, 2.2-mm-ID tip at drop-formation rates from 5 to 10 per minute. Data were collected with an automatically recording electronic balance (Sartorius, Model 1405 B MP8-1) and an IBM-PC. Measurement details and tension data are available elsewhere.[20]

Table 1 lists the equilibrium spreading coefficients of oil at the air/water interface, $S_{o/w}$ for several of the systems studied. If $S_{o/w}$ is positive, the oil spreads at the air/aqueous-surfactant-solution interface, whereas if $S_{o/w}$ is negative, the oil droplet forms a lens. All spreading behavior was verified by actual observation of the fate of an oil droplet entering the surfactant-solution/air interface.

Experiment Design.

The choice of chemicals and the manner in which the foam-flow experiments were performed minimized the possibility of any of the seven foam/oil destabilization mechanisms other than spreading. None of the surfactant/oil systems formed strong macroemulsions. Moreoever, the concentration of surfactant used in the experiments and the fact that all phases including the solid surfaces were pre-equilibrated precluded any foam destabilization as a result of surfactant depletion. Foam was pregenerated to ensure that the effect of oil on foam stability and not on foam generation was studied. The micromodel was strongly water-wet and remained so in the presence of the oils and surfactants.

Results and Discussion

Oil Spreading.

To verify the oil-spreading mechanisms for foam destabilization, the AOS 1416 surfactant system (no salt) was tested in the micromodel foam-flow apparatus against dodecane and hexane at ROS. For this case, Table 1 reports that dodecane is a spreading oil while hexane is nonspreading. Fig. 2 gives the pressure histories for both experiments (dodecane and hexane) and for foam introduction into an initially surfactant-solution-saturated, oilfree micromodel. In all three cases, the pressure drop eventually rises to a steady value at which point breakthrough of foam occurs. Steady-state foam mobilities in Fig. 2 are about a factor of 12 lower than that for water. The final pressure drops for hexane and dodecane are slightly above that for the oil-free medium because trapped oil reduces the pore space available for foam flow.

Fig. 2 shows that the presence of oil in the medium clearly has a major debilitating effect on foam stability. Both the pressure response and

breakthrough time are substantially faster in the oilfree experiment (Le., about 50 compared with 7 PV). This result confirms the deleterious effect of oil on foam stability in porous media noted by past researchers.

During the foam floods conducted, some oil was produced from the micromodel. The oil is initially present in the form of trapped blobs about the size of pore bodies. Upon foam injection, oil is produced by three modes: (1) foam bubble breakage induces emulsification of oil droplets whose size, compared with pore sizes, permits flow out of the medium; (2) oil fIlms or lenses form on the borders of foam bubbles and travel with them out of the medium; and (3) once a substantial pressure drop is established, large, whole oil blobs are dislodged and produced. The dominant mode of production roughly corresponds with the chronology of the foam flood. Mode 1 dominates at the outset of the foam flood while Mode 3 dominates in the later stages. The foam floods reduce the oil saturation in the model from 30 to ∼20%. Visual observations of the model after a complete foam flood reveal that the remaining oil exists in trapped blobs whose sizes now are on the order of the intermediate to smaller pore bodies.

The most important result shown in Fig. 2 is that both the pressure response and the breakthrough time occur more rapidly in the dodecane system than in the hexane system. This suggests that the nonspreading hexane actually destabilizes foam to a greater extent than the spreading dodecane. Obviously, this contradicts the oilspreading mechanism, which suggests that the AOS 1416 system should be stable, or at least more stable, against nonspreading hexane.

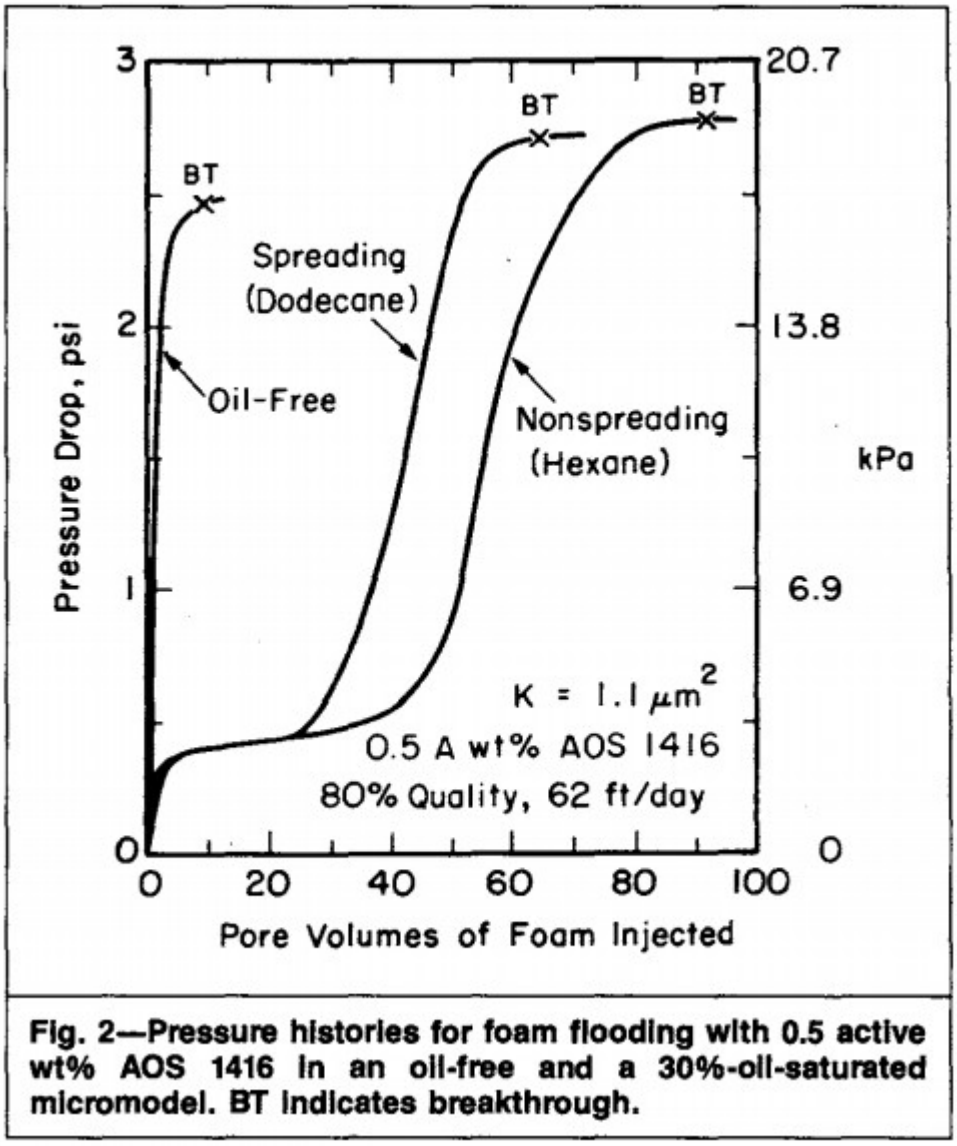

Fig. 2—Pressure histories for foam flooding with 0.5 active wt% AOS 1416 in an oil-free and a 30%-oil-saturated micromodel. BT indicates breakthrough.

Examination of Table 1 strikingly demonstrates that the foam stability gauged by the breakthrough time in the micromodel does not correlate with the spreading (or nonspreading) of the oil. Both the spreading coefficient and the breakthrough time were measured for several initially unequilibrated oil/aqueous-surfactant systems. No discernible difference was observed for either experiment. Local equilibration apparently occurs rapidly, even in laboratory time scales.

Additional information is available from the effect of insoluble oils on the stability of bulk foams. Many examples exist of nonspreading oils that perform excellently as antifoams.[21] Ross and McBain[22] list five examples of oils that exhibit negative spreading coefficients but are still rated as good antifoams. Sharovarnikov[23] found foam destruction upon addition of oils with both positive and negative spreading coefficients. Kruglyakov and Kotova[24]

and Frye[11] state that nonspreading oils seem to be more effective in collapsing bulk foam.

All these findings cast doubt on the generality of the oil-spreading mechanism of foam breakage in porous media. We must look elsewhere.

Destabilization by Pseudoemulsion-Film Breakage.

A painstaking search of the accumulated videomicrographs revealed that events before the spreading (or nonspreading) event have a major influence on foam stability. More specifically, the foam present in the micromodel remained stable to collapse when the pseudoemulsion films (water films between oil and gas) formed in the medium remained stable and vice versa. The stability of the pseudoemulsion films controlled foam stability, regardless of the subsequent spreading characteristics of the oil. This finding forms the basis of the pseudoemulsion-film foam-destabilization mechanism. Figs. 3 and 4 give visual evidence for this mechanism.

Fig. 3 displays a sequence of micromodel pore-level pictures taken of the AOS 1416/hexane (nonspreading) foam-flow experiment described in Fig. 2. In these micrographs, the various phases are differentiated by changes in brightness. The phases, labeled from lightest to darkest, are r (rock), 0 (oil), w (aqueous surfactant solution), and g (gas in the form of bubbles). Relative time is listed under each of the micrographs. Fig. 3a shows the formation of several pseudoemulsion films, the most important of which is located near the lower left corner of the photograph and noted by a dark arrow. Several stable foam lamellae also exist in this picture. Figs. 3b and 3c display the thinning process of the pseudoemulsion film mentioned previously. Thinning to breakage takes place in 7.3 seconds. Notice that, although the pseudoemulsion film has nearly thinned to collapse, the foam lamellae in the picture remain stable. Fig. 3d captures breakage of the pertinent pseudo-emulsion film. Fig. 3e, taken 1/30 second later, reveals collapse of the foam lamella closest to the broken pseudoemulsion film (i.e., 498 near the lower central portion of the micrograph). After another 1/30 second, several more lamellae in the picture are rendered unstable and break, as shown in Fig. 3f.

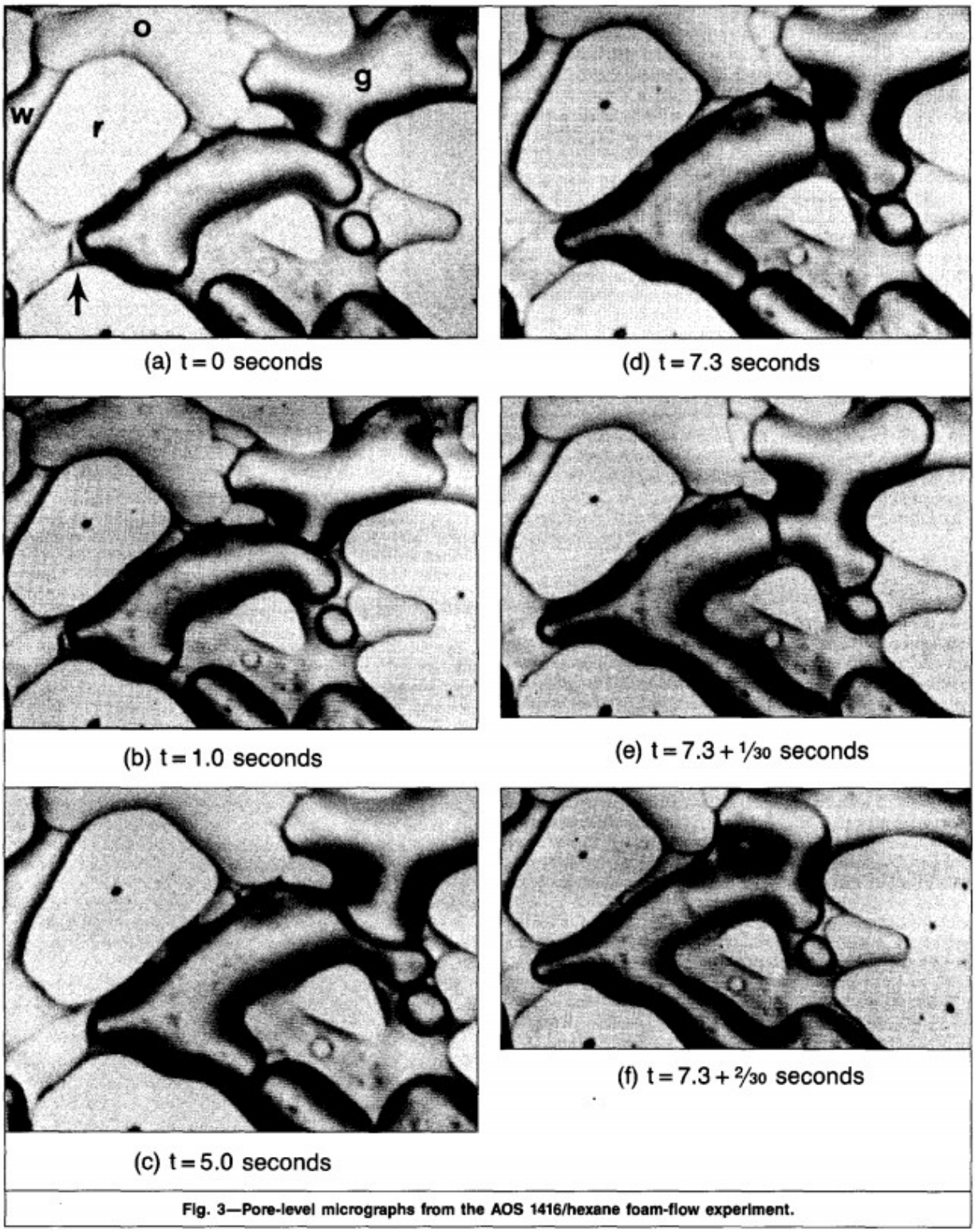

Fig. 3—Pore-level micrographs from the AOS 1416/hexane foam-flow experiment.

For our systems, the type of oil (spreading or nonspreading) has no effect on the foam-breakage process. Visually, all aspects of a spreading-oil experiment appear identical to a nonspreading oil. This is evidenced in Fig. 4, where a series of micrographs of the AOS 1416/dodecane (spreading)

foam-flow experiment in Fig. 2 are presented. Again, the various phases are labeled and relative time is listed below each photograph. The pseudoemulsion film of interest exists in the upper left portion of these pictures and is highlighted in Fig. 4a by a dark arrow. It is initially much thinner than that described in Fig. 3 and cannot be seen directly.

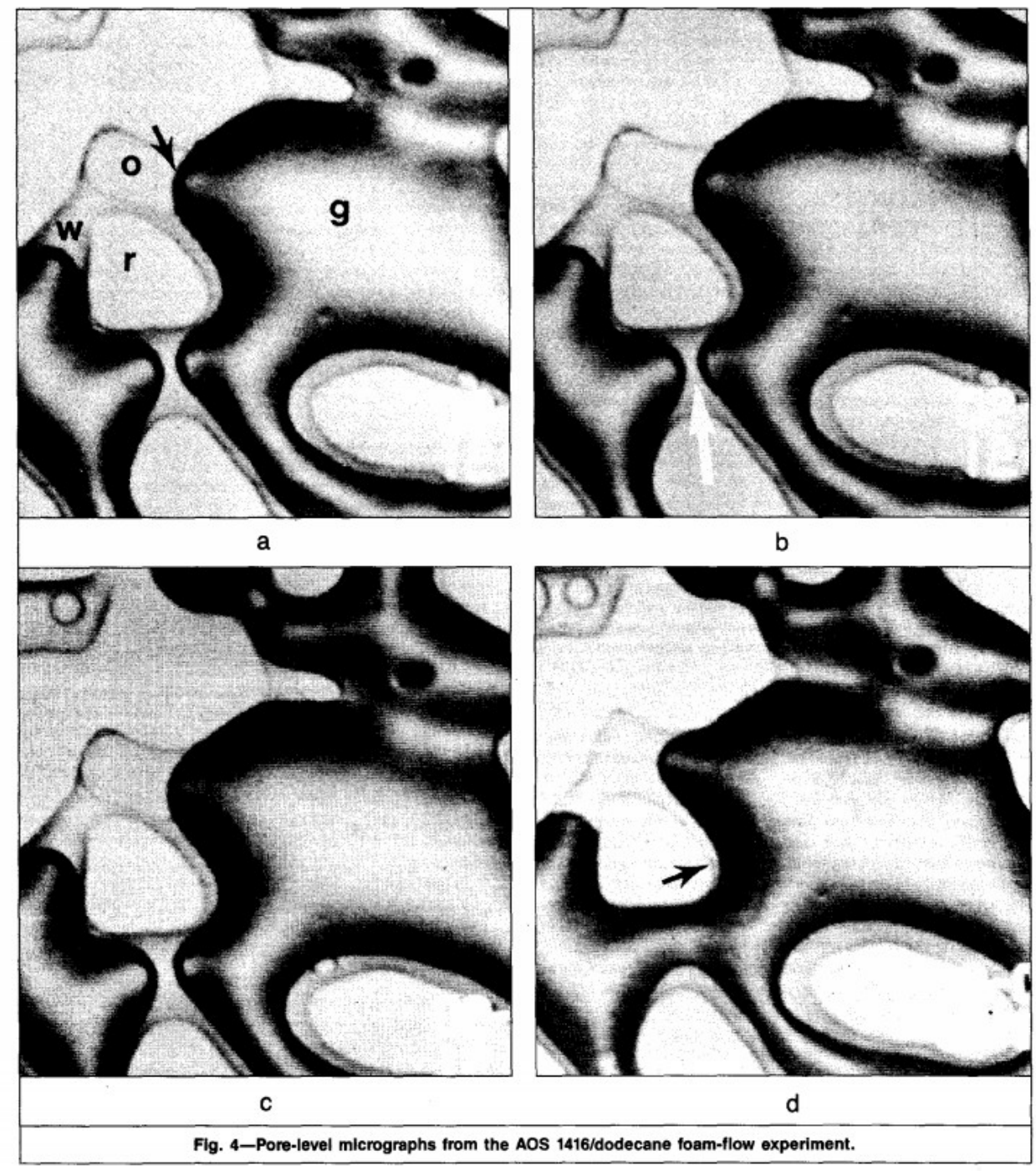

Fig. 4—Pore-level micrographs from the AOS 1416/dodecane foam-flow experiment.

Figs. 4a through 4c show the pseudoemulsion fIlm thinning above a thick aqueous pendular bridge separating two large gas bubbles (labeled by a

white arrow in Fig. 4b). Fig. 4d displays the breakage of the pseudoemulsion film and the subsequent foam bridge collapse. The thick water bridge quickly drained to a lamella and ruptured as a result of the pseudoemulsion-film breakage. Unfortunately, these events took place at a rate that exceeded the recording speed of the VCR. The time between pseudoemulsion-film breakage and foam-lamella rupture was < 1/30 second, precluding photographing both events separately. Notice from the dark arrow SPE Reservoir Engineering, November 1990 in Fig. 4d that the oil has spread macroscopically to the right and along the surface of the foam bubble. However, close analysis reveals that the oil did not have time to spread all the way to the foam bridge before it collapsed. Therefore, macroscopic spreading did not induce the lamella rupture. The pseudoemulsion film photographed in Fig. 4 thinned to rupture in 4.0 seconds.

The events in Figs. 3 and 4 are representative of a large number of visual observations made on the interactions between foam and oil in the etched-glass micromodel. For all the surfactants and oils studied, the pseudoemulsion-film destabilization mechanism was observed as the source of foam breakage by residual oil. Once the pseudoemulsion films break, surrounding foam lamellae collapse. Although primary, pseudoemulsion-film rupture must not be taken as the only way oil can destabilize foam. For example, after pseudoemulsion fllms of two nearby foam bubbles rupture, the resultant spreading oil or oil lenses can interact to destroy the intervening water fllm and thereby destroy the foam. This interaction is analogous to that pertinent for oil-in-water macroemulsions. Of course, with unequilibrated phases, any of the mechanisms that deplete the surfactant will destabilize the foam. Finally, the pseudoemulsion-fllm destabilization mechanism needs verification for a wide range of surfactants under more realistic conditions and with actual crude oils. We anticipate that it will remain a general phenomenon. One possible means for testing this assertion, and also for screening surfactants for stability against oil, is a 1:1 correspondence between foam breakthrough times from oil-laden cores and rest times for oil droplets at the gas/aqueous surfactant interface.[20]

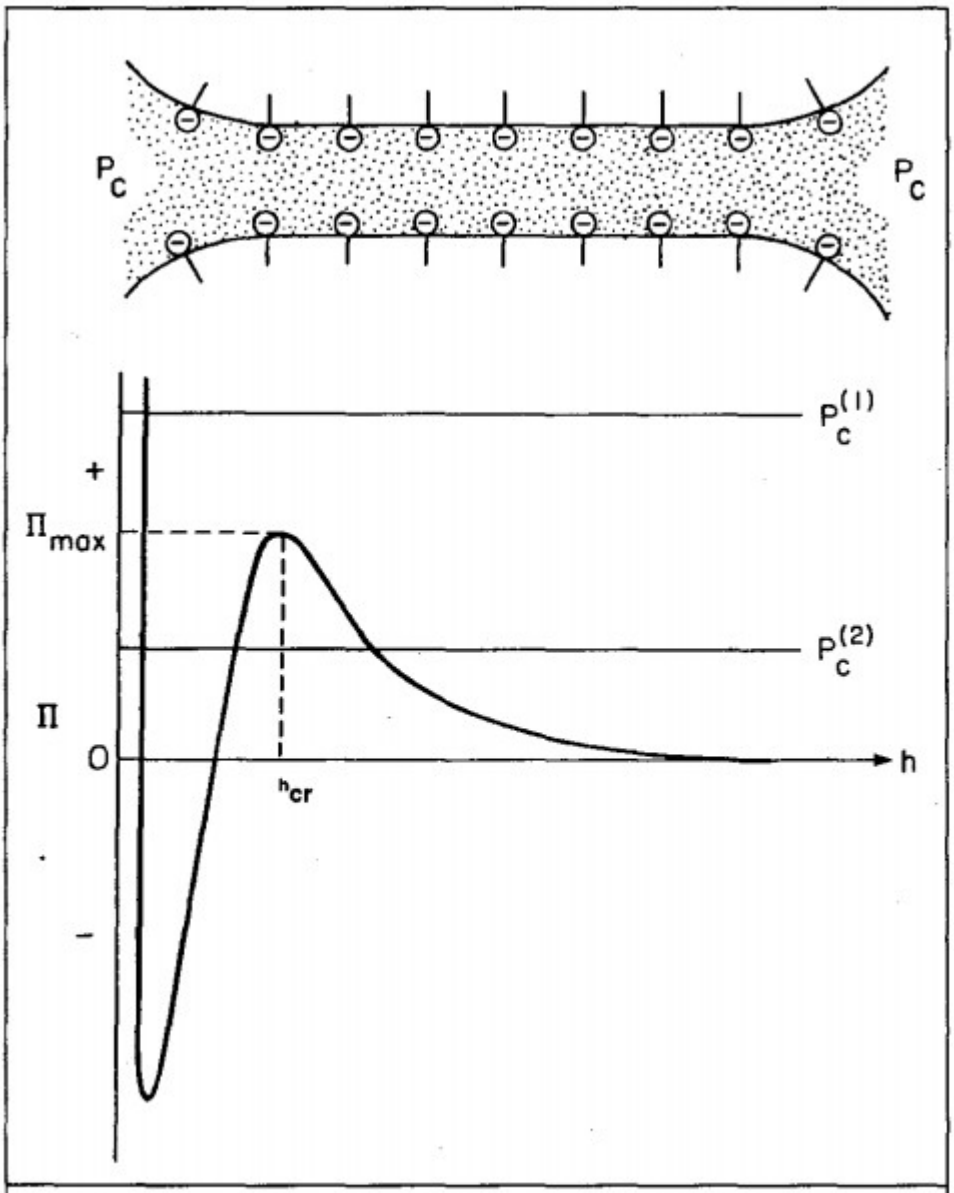

Fig. 5—A conjoining/disjoining-pressure isotherm and the capillary pressures necessary for an unstable, $P_c^{(1)}$, and metastable, $P_c^{(2)}$, foam or pseudoemulsion film.

Pseudoemulsion-Fllm Drainage and Collapse.

We quantify the pseudoemulsion-fllm rupture times measured in Figs. 3 and 4 in this section. Pseudoemulsion and foam fllms in wetting-liquid, partially saturated porous media are drained (or possibly filled) by capillary suction forces.[12,19] If no other forces are operative, such fllms cannot exist. However, liquid fllms that contain surfactants that are less than about 1 μm thick are subject to nonbulk attractive and repulsive intermolecular forces called conjoining and disjoining pressures.[25] Conjoining/disjoining forces are a direct

function of the fIlm thickness and a strong indirect function of the surfactant formulation. Fig. 5, shows a characteristic conjoining/disjoining pressure isotherm, II, as a function of the film (foam or pseudoemulsion) thickness, *h*. Not all fIlm thicknesses are stable, even to infinitesimal thermal perturbations. Vrij[26] showed that when $\delta\Pi/\delta h > 0$, the fIlm is unstable. The molecular-thickness films in Fig. 5, where strongly repulsive structural forces are thought to dominate, are very unlikely during flow through porous media. Therefore, the Vrij analysis demands that metastable fIlms can exist only for $h > h_{er}$. Lamellae or pseudoemulsion films of thickness greater than h_{cr} are metastable, rather than completely stable, because large-scale disturbances eventually will destroy them to reduce the overall surface area.

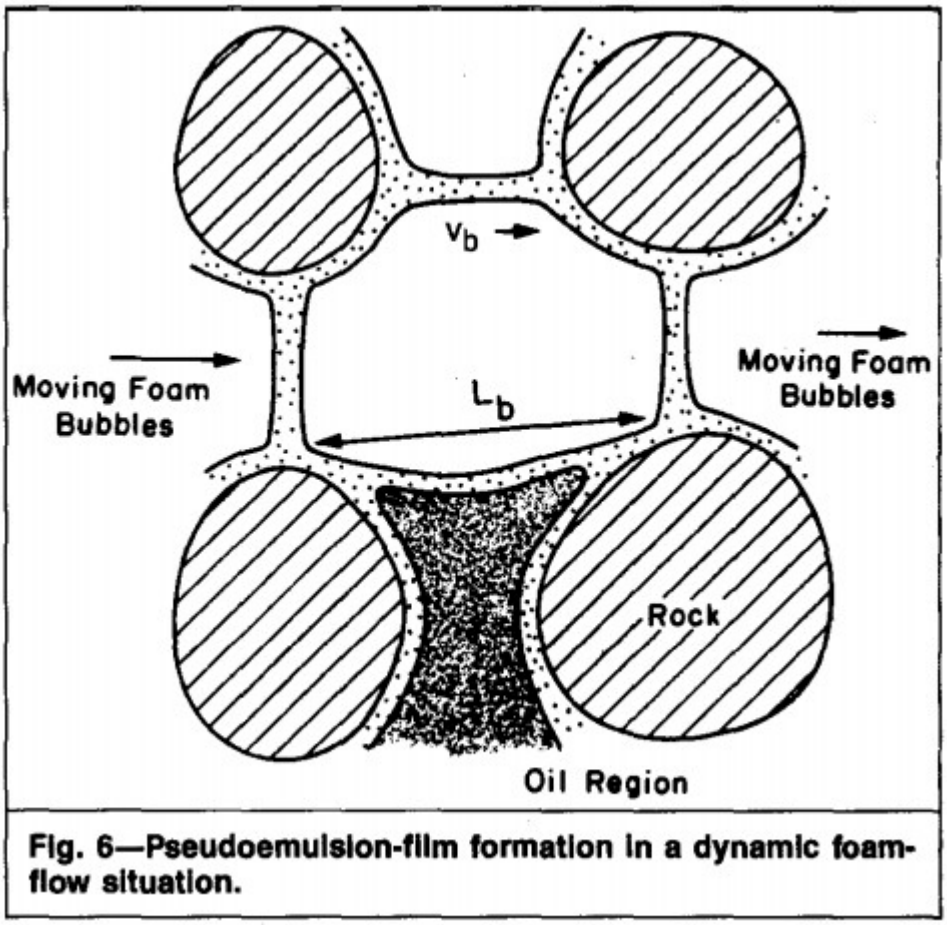

Fig. 6—Pseudoemulsion-film formation in a dynamic foam-flow situation.

Fig. 5 also shows two values of the porous-medium capillary pressure, P_c. For a relatively dry medium with a large capillary suction pressure, $P_c^{(1)}$, the film drains to h_{cr} and then ruptures. For a wetter medium at $P_c^{(2)}$, however, the fIlm can establish a metastable equilibrium state with P_c=II. Whether a particular pseudoemulsion or foam fIlm can attain equilibrium depends primarily on the surfactant design as reflected in the value of Π_{max}. Whenever P_c and II are not in balance, the film drains or fills to establish equilibrium

except when h falls below h_{cr}, where breakage occurs. Thus, the driving force for liquid exchange in thin fIlms is P_c - II.

Because thin-fIlm rupture times are typically faster than drainage times,[12] the overall breakage times in Figs. 3 and 4 may be calculated from the drainage rates. We adopt the simple plane-parallel model of Reynolds for inextensible surfaces[27]:

$$-(dh/dt)=(\pi h^3/3\mu A_c)(P_c-\Pi). \quad \ldots\ldots\ldots\ldots\ldots\ldots\ldots (1)$$

Manlowe[20] argues that for the pseudoemulsion films in the micromodel, the appropriate capillary suction pressure is that for the gas and water phases. It remains to determine an expression for II representative of pseudoemulsion films.

We write the conjoining/disjoining pressure as a sum of two terms[28]:

$$\Pi=-A_H/h^3+\tfrac{1}{2}[Q_g^2+Q_o^2+2Q_gQ_o\cosh(\kappa h)]\sinh^2(\kappa h)/\epsilon, \quad \ldots\ldots\ldots\ldots\ldots\ldots\ldots\ldots\ldots\ldots (2)$$

where Q_i = surface charge density of the ith interface against water. The first term on the right side of this expression corresponds to the attractive dispersion or Hamaker forces,[29] with A_H denoting the Hamaker constant.[30-32] The second term on the right of Eq. 2 corresponds to the repulsive overlap of constant-charge electrostatic double layers[33] and originates from adsorption of the anionic surfactants. κ is the inverse Debye length defined for symmetric z-z electrolytes as

$$\kappa^2\equiv 2z^2e^2N_AC_\infty/\epsilon kT. \quad \ldots\ldots\ldots\ldots\ldots\ldots\ldots\ldots (3)$$

Eqs. 1 and 2 are combined and solved numerically for thinning from an initial thickness, h_0, until h_{cr} is reached, which defines the drainage time or, equivalently, the collapse time, t_d. Fortunately, for values of κh_0 greater than ~3, the drainage time is independent of the initial thickness.

To establish absolute theoretical drainage times, a number of physical parameters must be determined: A_H, P_c, κ, A_c, Q_8, and Q_0. Eq. 3 specifies the dependence of κ on total electrolyte concentration. For the experimental systems in this research (excluding those with brine), $1/\kappa$ is ~7.5 nm. Estimates of Hamaker constants for systems similar to ours are quite numerous in the literature[34] and typically range between 10^{-20} and 5×10^{-20} J. The drainage capillary pressure, P_c = 6.9 kPa, was estimated by interpolating the two-phase capillary-pressure/water-saturation data of Khatib et at.[19] for porous media with permeabilities of 1.1 μm^2. Studies on the surfactant sodium dodecyl sulfate indicate that surface charges for gas/water and oil/water interfaces span values from 0.02 to 0.1 μC/cm^2.[34] For lack of a better estimate, we adopted this range. The area of contact, A_c, is set at 2.5×10^3 μm^2 based on that of the pseudoemulsion film in Fig. 3.

Given these estimated parameter values, we calculate an absolute drainage time of 7.0 seconds. This compares well with the observed collapse times in Figs. 3 and 4 of 7.3 and 4.0 seconds, respectively. Unfortunately, lack of precise surface-charge densities precludes exact comparison of theory and data because drainage times are very sensitive to those values. Nevertheless, this calculation confirms the basic physics that the pseudoemulsion-filmcollapse process results from capillary pressure suction overcoming the repulsive disjoining force of the stabilizing surfactant.

Ramifications of Pseudoemulslon-Fllm Foam Destabilization

By letting an oil drop rise through the surfactant solution and reside at the air/water interface, we find that the pseudoemulsion films collapse within about 1 minute for all the surfactant/oil systems studied.[20] Accordingly, in the language of Fig. 5, all the surfactants in this work form unstable pseudoemulsion films. It is therefore perplexing why steady state is ever achieved in the foam displacements of residual oil in Fig. 2. After a decrease in oil content of only about 5 to 10 saturation units, foam is able to propagate. One possible explanation relies on the concept of dynamic metastability of pseudoemulsion films explained below.

A pseudoemulsion film forms during dynamic foam flow when a gas bubble contacts oil. Fig. 6 depicts pseudoemulsion-film formation during flow, where v_b is the local pore-level velocity of the bubble and L_b is its length. As a lamella rides over the residual oil blob, it deposits a pseudoemulsion film of thickness h_0. This pseudoemulsion film drains under capillary suction from surrounding liquid-filled nooks, crannies, or pores. Drainage continues until either the ensuing lamella lays down a new film or the thickness of the original pseudoemulsion-film portion near the beginning of the oil contact falls to h_{cr}, initiating rupture. Which of these two events actually occurs depends on the magnitudes of the residence and drainage times of the differential section of the pseudoemulsion located at the oil-contact front.

The residence or contact time follows directly from the bubble length and velocity:

$$t_c = L_b / v_b. \quad \ldots\ldots\ldots\ldots\ldots\ldots\ldots\ldots\ldots\ldots\ldots\ldots\ldots\ldots\ldots\ldots (4)$$

For times longer than t_c, a new plateau border traverses the oil contact, regenerating the pseudoemulsion film. Provided that redistribution of liquid by convection along the film is negligible [i.e., provided that $\sigma_{gw}/\kappa L_b^2 (P_c - \Pi_{\max}) << 1$], and because film drainage rates are insensitive to h_0, the characteristic drainage time to rupture of the differential slice of pseudoemulsion fIlm follows from Eq. 1:

$$t_d \sim \mu/\kappa^2 A_c (P_c - \Pi_{\max}), \quad \ldots\ldots\ldots\ldots\ldots\ldots\ldots\ldots\ldots\ldots (5)$$

where $1/\sqrt{A_c}$ is now interpreted as the local drainage area per unit volume of fIlm. Note the strong dependence of t_d on the surfactant formulation embodied in II_{max}.

A pseudoemulsion fIlm will rupture and consequently break surrounding foam lamellae only when its drainage time is less than the time of contact with the oil. Stated mathematically, we have unstable foam for $t_c/t_d > 1$ and dynamically metastable foam for $t_c/t_d < 1$. Thus, it is possible for unstable pseudoemulsion fIlms (i.e., those with $P_c > II_{max}$) to remain in existence during flow and not to destroy the foam. This is the concept of dynamic metastability of foam against oil in porous media.

The proposed explanation for steady state in Fig. 2 is as follows. The smaller amount of oil after the foam flood, compared with that after the waterflood, reduces the number of oil contacts with the foam bubbles. This reduces the coalescence rate and minimizes coarsening of bubble texture. Therefore, as verified visually, the average value of L_b is smaller, Hence, from Eq. 4, the contact time is lowered enough so that t_c/t_d falls below unity, creating dynamically stable pseudoemulsion fIlms. Stable foam can now propagate.

The idea of a dynamically metastable foam is a main rarnification of the proposed pseudoemulsion-film foam-destabilization mechanism. It also appears possible to extend this idea to predict the actual kinetic rate of oil destabilization of foam in porous media. [20] Finally, if indeed pseudoemulsion-film stability is the paramount underpinning of foam stability against oil in porous media, then surfactant packages should be so formulated. Molecularly, a more stable pseudoemulsion film translates into a larger value of the maximum conjoining/disjoining pressure, II_{max}.

Conclusions

For the seven commercial anionic surfactants and two alkane oils in this study, both pre-equilibrated and unequilibrated, there is no correlation between oil spreading and foam stability in a strongly water-wet, etched glass micromodel of Kuparuk sandstone containing residual oil. Rather, we find that foam stability in porous media is governed by the stability of the liquid films formed between foam bubbles and oil (pseudoemulsion films). Direct visual evidence from the transparent micromodel shows convincingly that rupture of foam lamellae is induced by the collapse of pseudoemulsion films. Because pseudoemulsion-film rupture must precede either oil spreading or lens formation, it appears to be a general destabilization mechanism. Pseudoemulsion-film drainage times calculated from the simple Reynolds theory are in good agreement with values measured in the porous-medium micromodel, confirming the basic physics of the pseudoemulsion-fIlm-rupture process.

The concept of a dynamically metastable foam in the presence of oil is introduced, grounded on the proposed pseudoemulsionfIlm destabilization

mechanism. This concept permits an explanation of how foam lamellae that are unstable to oil can remain stable during flow through oil-laden porous media. Surfactant formulation for foam insensitivity to oil in porous media should be based on stabilizing pseudoemulsion films.

Nomenclature

A_c = area of contact between oil and foam bubble, m^2
A_H = Hamaker constant, J
C_∞ = total bulk concentration of all solution electrolytes, $kmol/m^3$
e = elementary charge, C
h = thickness of pseudoemulsion film, m
h_{cr} = film thickness corresponding to maximum conjoining/disjoining pressure, m
h_0 = initial film thickness, m
k = Boltzmann's constant, J/K
L_b = length of gas bubble, m
N_A = Avogadro's number, mol^{-1}
P_c = capillary pressure, Pa
Q_i = surface charge of ith interface against water, C/m^2
$S_{o/w}$ = spreading coefficient for oil on water, N/m
t_c = time of contact between foam bubble and oil blob, seconds
t_d = pseudoemulsion-film drainage time, seconds
T = temperature, K
v_b = local pore-level velocity of bubbles, m/s
z = valence of ions
ϵ = permittivity constant, $C^2/J \cdot m$
κ = inverse Debye length, m^{-1}
μ = viscosity, $Pa \cdot s$
Π = conjoining/disjoining pressure, Pa
σ_{ij} = interfacial tension between ith and jth phases, N/m

Subscripts

cr = critical
g = gas (air)

max = maximum
o = oil
w = surfactant solution

Superscripts
(1) = State 1
(2) = State 2

Acknowledgments

This work was supported by V.S. DOE Grant DE-AC03- 76SFOOO98 to the Lawrence Berkeley Laboratory of the V. of California. Manlowe gratefully acknowledges a fellowship from the Regents of the V. of California.

References

1. Holm, L.W.: "Foam Injection Test in the Siggins Field, illinois," JPT (Dec. 1970) 1494-1506.

2. Dilgren, R.E., Deemer, A.R., and Owens, K.B.: "The Laboratory Development and Field Testing of Steam/Noncondensible Gas Foams for Mobility Control in Heavy Oil Recovery," paper SPE 10774 presented at the 1982 SPE California Regional Meeting, San Francisco, March 24-26.

3. Ploeg, J.F. and Duerksen, J.H.: "Two Successful Steam/Foam Field Tests, Sections 15A and 26C, Midway-Sunset Field," paper SPE 13609 presented at the 1985 SPE California Regional Meeting, Bakersfield, March 27-29.

4. Mohammi, S.S., Slyke, D.C., and Ganong, B.: "Steam-Foam Pilot Project in Dome-Tumbador, Midway-Sunset Field," SPERE (Feb. 1989) 7-16.

5. Patzek, TJ. and Koinis, M.T.: "Kern River Steam-Foam Pilots," JPT (April 1990) 496-503.

6. Fried, A.N.: "The Foam-Drive Process for Increasing Recovery of Oil," RI 5866, USBM, Washington, DC (1961).

7. Mast, R. F.: "Microscopic Aspects of the Behavior of Foam in Porous Media," paper SPE 3997 presented at the 1972 SPE Annual Meeting, San Antonio, Oct. 8-11.

8. Kanda, M.: "Mechanism of Foam Formation in Porous Media," PhD dissertation, U. of Texas, Austin (1976).

9. Lau, H.C. and O'Brien, S.M.: "Surfactant Transport Through Porous Media in Steam-Foam Processes," SPERE (Nov. 1988) 1177-85.

10. Nikolov, A.D. et al.: "The Effect of Oil on Foam Stability: Mechanisms and Implications for Oil Displacement by Foam in Porous Media," paper SPE 15443 presented at the 1986 SPE Annual Technical Conference and Exhibition, New Orleans, Oct. 5-8.

11. Frye, G.: "Interactions Between Surface Active Components in the Promotion imd Destruction of Foams, " PhD dissertation, U. of Washington, Seattle (1987).

12. Jimenez, A.!, and Radke, C.J.: "Dynamic Stability of Foam Lamellae. Flowing Through a Periodically Constricted Pore," Oil-Field Chemistry; Enhanced Recovery and Production Stimulation, J .K. Borchardt and T.F. Yen (eds.), ACS Symposium Series 396, American Chern. Soc., Washington, DC (1989) Chap. 25, 461-79.

13. Borchardt, J .K. et al.: "Surfactants for CO2 Foam Flooding," paper SPE 14394 presented at the 1985 SPE Annual Technical Conference and Exhibition, Las Vegas, Sept. 22-25.

14. Ransohoff, T.C. and Radke, C.J.: "Mechanism of Foam Generation in Glass-Bead Packs," SPERE (May 1988) 573-85. 502

15. Ginley, G.M. and Radke, C.J.: "The Influence of Soluble Surfactants on the Flow of Long Bubbles Through a Cylindrical Capillary," OilField Chemistry; Enhanced Recovery and Production Stimulation, J.K. Borchardt and T.F. Yen (eds.), ACS Symposium Series 396, American Chern. Soc., Washington, DC (1989) Chap. 26, 481-501.

16. Bernard, G.G. and Holm"L.W.: "Effect of Foam on Trapped Gas Saturation and on Permeability of Porous Media to Water," SPEJ (Dec. 1965) 295-300; Trans., AIME, 234.

17. Lau, H.C. and O'Brien, S.M.: "Effects of Spreading and Nonspreading Oils on Foam Propagation Through Porous Media, " SPERE (Aug. 1988) 893-96. '

18. Jensen, J.A. and Friedmann, F.: "Physical and Chemical Effects of an Oil Phase on Propagation of Foam in Porous Media," paper SPE 16375 presented at the 1987 SPE California Regional Meeting, Ventura, April 8-10.

19. Khatib, Z.I., Hirasaki, G.J., and Falls, A.H.: "Effects of Capillary Pressure on Coalescence and Phase Mobilities in Foams Flowing Through Porous Media," SPERE (Aug. 1988) 919-26.

20. Manlowe, DJ.: "Pore-Level Mechanisms of Foam Destabilization by Oil in Porous Media," MS thesis, U. of California, Berkeley (1988).

21. Tsuge, H., Ushida, J., and Hibino, S.: "Measurement of Film-Breaking Ability of Antifoaming Agents," J. Colloid Interface Sci. (1984) 100, No.1, 175-90.

22. Ross, S. and McBain, J.W.: "Inhibition of Foarning Solvents Containing Known Foamers," Ind. & Eng. Chem. (1944) 36, 570-88.

23. Sharovarnikov, A.F.: "Mechanism of the Contact Destruction of Foams by Organic Solvents," Colloid J. (1982) 45, No.3, 548-57.

24. Kruglyakov, P.M. and Kotova, T. T.: "Role of Antifoam Agent Spreading in Chemical Foam Suppression," Dok. Phys. Chem. (1969) 188, No.4, 187-201.

25. Deljaguin, B. V.: "Interaction of Particles Carrying Double Electrical Layers and of Aggregative Stability of Lyophobe Colloids and Disperse Systems," Zhur. Fis. Khim. (1940) 14, 137-51.

26. Vrij, A.: "Possible Mechanisms for the Spontaneous Rupture of Thin Free Liquid Films," Disc. Faraday Soc. (1966) 42, 23-33.

27. Reynolds, 0.: "On the Theory of Lubrication and Its Application to Mr. Beauchamp Tower Experiment," Trans. Ruy. Phil. Soc., London (1886) A177, 157-324.

28. Liftshitz, V.G.: "The Theory of Molecular Attractive Forces Between Solids," Soviet Physics JEPT (1956) 2, 73-83.

29. Hamaker, H.C.: "The London Van der Waals Attraction Between Spherical Particles," Physica (1937) 4, 1058-72.

30. Levine, S. and Bell, G.M.: "An Extension of the Stability Theory of Lyophobic Colloids," J. Colloid Interface Sci. (1962) 17, 835-56.

31. Burrill, K.A. and Woods, D.R.: "Film Shapes for Deformable Drops at Liquid-Liquid Interfaces ill: Drop Rest Times," J. Colloid Interface Sci. (1973) 42, No.1, 35-51.

32. Mohanty, K.K.: "Fluids in Porous Media: Two-Phase Distributions and Flow," PhD dissertation, U. of Minnesota, Minneapolis (1981).

33. Oshima, H., Makino, K., and Kondo, T.: "Electrostatic Interactions of Two Parallel Plates with Surface Charge Layers," J. Colloid Interface Sci. (1987) 116, No.1, 196-99.

34. Malhotra, A.K. and Wasan, D.T.: "Effect of Film Size on Drainage of Foam Films and Emulsion Films," AIChE J. (1987) 39, No.9, 1533-41.

35. Heiba, A.: "Porous Media: Fluid Distributions and Transport with Applications to Petroleum Recovery, " PhD dissertation, U. of Minnesota, Minneapolis (1985).

SI Metric Conversion Factors

Å	× 1.0*	E−01	=	nm
Btu	× 1.055 056	E+00	=	kJ
dynes/cm	× 1.0*	E+00	=	mN/m
ft	× 3.048*	E−01	=	m
°F	(°F−32)/1.8		=	°C
in.	× 2.54*	E+00	=	cm
psi	× 6.894 757	E+00	=	kPa

*Conversion factor is exact.